

## Early Response Assessment Using 3'-Deoxy-3'-[<sup>18</sup>F]Fluorothymidine-Positron Emission Tomography in High-Grade Non-Hodgkin's Lymphoma

Ken Herrmann,<sup>1</sup> Hinrich A. Wieder,<sup>1,2</sup> Andreas K. Buck,<sup>1</sup> Marion Schöffel,<sup>3</sup> Bernd-Joachim Krause,<sup>1</sup> Falko Fend,<sup>4</sup> Tibor Schuster,<sup>5</sup> Christian Meyer zum Büschenfelde,<sup>3</sup> Hans-Jürgen Wester,<sup>1</sup> Justus Duyster,<sup>3</sup> Christian Peschel,<sup>3</sup> Markus Schwaiger,<sup>1</sup> and Tobias Dechow<sup>3</sup>

**Abstract Purpose:** To evaluate 3'-deoxy-3'-[<sup>18</sup>F]fluorothymidine-positron emission tomography (FLT-PET) for early monitoring response of high-grade non-Hodgkin's lymphoma to treatment with cyclophosphamide-adriamycin-vincristine-prednisone chemotherapy with or without rituximab immunotherapy (R-CHOP/CHOP).

**Experimental Design:** Twenty-two patients with histologically proven high-grade non-Hodgkin's lymphoma scheduled to undergo first line treatment with R-CHOP/CHOP were included. All patients received baseline imaging before therapy with FLT-PET. For noninvasive assessment of treatment response, FLT-PET was repeated at following time points: group 1 ( $n = 6$ ), 1 and 6 weeks after R-CHOP/CHOP; group 2 ( $n = 16$ ), 2 days after rituximab and 2 days after CHOP application. Emission images were acquired 45 min after injection of 300 to 370 MBq of FLT. FLT uptake was quantified by region-of-interest technique on a lesion basis. Maximum standardized uptake values (SUV) for FLT were calculated using circular region of interest (diameter, 1.5 cm).

**Results:** In all patients, morphologically proven lesions showed initially high FLT uptake (mean SUV,  $8.1 \pm 3.9$ ). In group 1, mean FLT SUV decreased 7 days after R-CHOP/CHOP by 77% ( $P < 0.001$ ), the reduction in FLT SUV from baseline was 85% after 40 days ( $P = 0.003$ ). In group 2, FLT uptake in patients without dexamethasone pretreatment revealed no significant reduction after rituximab ( $P = 0.3$ ) but significantly decreased 2 days after CHOP to 32% compared with the baseline value ( $P = 0.004$ ).

**Conclusions:** Administration of R-CHOP/CHOP is associated with an early decrease in lymphoma FLT uptake. Interestingly, there was no reduction of FLT uptake after rituximab alone, indicating no early antiproliferative effect of immunotherapy. FLT-PET seems to be promising for early evaluation of drug effects in lymphoma.

The standard therapy for high-grade non-Hodgkin's lymphoma is cyclophosphamide-adriamycin-vincristine-prednisone (CHOP) or CHOP-like regimens. The introduction of the chimeric monoclonal anti-CD20 antibody rituximab to standard chemotherapy has been shown to significantly improve both event-free as well as overall survival (1, 2). In contrast to its role in combination therapies, rituximab itself does not

reveal a major cytotoxic effect as a single agent on high-grade non-Hodgkin's lymphoma (3).

To evaluate antitumor efficacy and possible mechanisms of action *in vivo*, therapy monitoring plays a major role for evaluation of new therapeutic approaches. For the last decades, helical computed tomography (CT) has represented the gold standard for staging and restaging of non-Hodgkin's lymphoma. However, definition of response criteria based on conventional radiographic characteristics remains difficult because patients treated with chemotherapy often present with residual masses of uncertain significance. Especially differentiation between fibrotic tissue and viable tumor by CT is only of limited accuracy (4–10).

Positron emission tomography using the glucose analogue 2-[<sup>18</sup>F]fluoro-2-deoxy-D-glucose (FDG) as a biomarker has been shown to significantly enhance the sensitivity in detection of malignant lymphoma in lymphatic tissue and extranodal manifestation sites (11–13). Interim FDG-positron emission tomography (PET) as early as one to two cycles after initiation of chemotherapy proved to be an accurate and independent predictor of progression-free survival and overall survival (14). Furthermore, residual FDG uptake after completion of

**Authors' Affiliations:** Departments of <sup>1</sup>Nuclear Medicine, <sup>2</sup>Radiology, <sup>3</sup>Internal Medicine III, and <sup>4</sup>Pathology, and <sup>5</sup>Institute for Medical Statistics and Epidemiology, Technische Universität München, Munich, Germany

Received 12/22/06; revised 2/28/07; accepted 3/29/07.

The costs of publication of this article were defrayed in part by the payment of page charges. This article must therefore be hereby marked *advertisement* in accordance with 18 U.S.C. Section 1734 solely to indicate this fact.

**Note:** K. Herrmann and H.A. Wieder contributed equally to this work.

**Requests for reprints:** Ken Herrmann, Department of Nuclear Medicine, Technische Universität München, Ismaningerstrasse 22, D-81675 Munich, Germany. Phone: 49-89-4140-2962; Fax: 49-89-4140-4950; E-mail: ken.herrmann@web.de.

©2007 American Association for Cancer Research.  
doi:10.1158/1078-0432.CCR-06-3025

chemotherapy revealed to be a strong predictor for disease recurrence and more accurate for diagnosis of relapse than conventional imaging (15–17). These data resulted in new guidelines making FDG-PET part of the routine workup in lymphoma patients (18–20).

Nevertheless, FDG is not tumor specific and can also accumulate in inflammatory lesions such as tuberculosis (granulomas), abscesses, and sarcoidosis (21, 22). To increase specificity for malignant lesions, other tracers that complement the information provided by FDG are required. Proliferative activity has been shown to be more specific for malignant tumors compared with an increase of glucose metabolism (23). Therefore, measurement of tumor growth and DNA synthesis *in vivo* might be appropriate for staging and assessment of response to therapy in malignant tumors.

[<sup>11</sup>C]Thymidine was the first PET tracer for noninvasive imaging of tumor proliferation, but its short half-life and its rapid metabolism *in vivo* make it less suitable for routine use. Recently, the thymidine analogue 3'-deoxy-3'-[<sup>18</sup>F]fluorothymidine (FLT), which is derived from the cytostatic drug azidovudine, has been reported as a stable PET tracer that accumulates in proliferating tissues and malignant tumors (24). Thymidine kinase 1 was revealed as a key enzyme responsible for the intracellular trapping of FLT (25, 26). Several human studies recently showed a significant correlation of tumoral proliferation and FLT uptake in lymphoma and other solid tumors including lung cancer, soft tissue sarcomas, and breast cancer (27–32). Imaging proliferative activity with FLT-PET has also been shown to be a sensitive tool for noninvasive assessment of tumor grading (27, 29, 33). In a recently published study, a cutoff value of FLT standardized uptake values (SUV) = 3 reliably differentiated between indolent and aggressive lymphoma (27).

Regarding therapy monitoring, significant decrease of FLT uptake was observed in animal models already 48 h after chemotherapy (25, 34, 35). In this study, we evaluated FLT-PET for early assessing response of high-grade non-Hodgkin's lymphoma to rituximab immunotherapy combined with CHOP chemotherapy (R-CHOP) or CHOP chemotherapy alone.

## Materials and Methods

**Patient population.** Twenty-two patients with biopsy-proven high-grade non-Hodgkin's lymphoma were included in this prospective study (16 men and 6 women; mean age, 59 ± 14 years). All patients were scheduled to undergo systemic chemotherapy with R-CHOP (*n* = 20) or CHOP (*n* = 2, patient nos. 19 and 22, both with anaplastic T-cell non-Hodgkin's lymphoma). Patient characteristics are shown in Table 1. FLT-PET was done before and during therapy. A total of 57 FLT-PET scans were done (9 patients with two scans and 13 patients with three scans; Table 1). Exclusion criteria were previous malignancies or preceding chemotherapy or radiotherapy, and age younger than 18 years. Details of the study were explained by a physician and written informed consent was obtained from all patients. The study protocol was approved by the local ethics committee of the Technische Universität München.

**Histologic classification.** Histology of lymphomas was classified according to the updated WHO classification system (36). In all 22 patients, histopathology revealed aggressive non-Hodgkin's lymphoma (Table 1), including 18 patients with diffuse large B-cell non-Hodgkin's lymphoma, 2 patients with grade 3 follicular lymphoma, and 2 patients with anaplastic T-cell non-Hodgkin's lymphoma.

**Treatment protocol.** All patients received CHOP in standard doses (cyclophosphamide 750 mg/m<sup>2</sup> day 1, doxorubicin 50 mg/m<sup>2</sup> day 1, vincristine 1.4 mg/m<sup>2</sup> day 1, and prednisone 100 mg day 1-5) every 3 weeks with dose modification or delays depending on blood counts.

**Table 1.** Patient characteristics: uptake of FLT in malignant lymphoma before (baseline) and during therapy as well as response to therapy

Patient	Age (y)	Histology	Clinical stage	Day 0	Day 2	Day 4	Day 7	Day 40	Response*
1	51	DLBCL	IBE	2.6	2.5	1.0	—	—	CR
2	69	DLBCL	IVAE	8.5	6.6	2.8	—	—	PR
3	76	DLBCL	IAE	11.8	10.4	—	—	—	PR
4	29	DLBCL	IAE	4.7	4.9	—	—	—	CR
5	71	DLBCL	IAE	19.4	16.3	3.0	—	—	PR
6	76	DLBCL	IAE	13.8	10.4	—	—	—	CR
7	27	DLBCL	IAE	8.0	7.8	1.8	—	—	CR
8	62	DLBCL	IIIAE	8.3	8.2	3.1	—	—	PR
9	55	DLBCL	IA	10.5	11.5	—	—	—	CR
10	69	DLBCL	IVA	14.8	14.3	9.0	—	—	PD
11	65	DLBCL	IAE	6.9	6.5	—	—	—	—
12	63	FL grade 3	IVA	7.6	2.1	—	—	—	CR
13	55	DBLCL	IA	7.2	2.7	—	—	—	PR
14	74	DBLCL	IA	5.8	6.2	1.5	—	—	CR
15	69	DBLCL	IA	7.7	10.6	1.4	—	—	CR
16	76	DLBCL	IAE	6.9	—	—	1.8	1.4	CR
17	48	DLBCL	IAE	8.2	—	—	2.0	1.0	CR
18	46	FL grade 3	IVAE	4.7	—	—	1.4	0.7	CR
19	34	Anaplastic T-cell	IIIA	6.2	—	—	1.0	0.8	CR
20	63	DLBCL	IAE	5.8	2.4	2.1	—	—	CR
21	70	DLBCL	IVAE	5.1	—	—	1.3	—	PR
22	56	Anaplastic T-cell	IIIA	4.6	—	—	0.7	—	CR

Abbreviations: DLBCL, diffuse large B-cell lymphoma; FL, follicular lymphoma; CR, complete response; PR, partial response; PD, progressive disease.

\*Response after completion of six cycles of R-CHOP/CHOP.

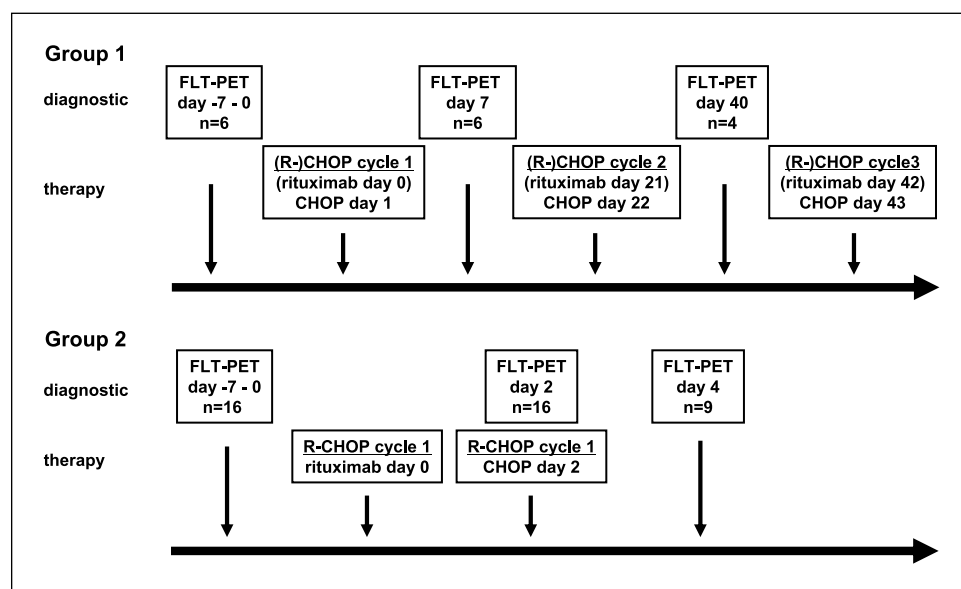


**Fig. 1.** Study design: diagram of the two different treatment groups and the respective FLT-PET schedules. Patients in group 1 were evaluated at baseline, on day 7, and before the beginning of the third cycle of R-CHOP/CHOP on day 40. In group 2, FLT-PET scans were done at baseline, 2 d after rituximab administration (CHOP was given the same day), and 2 d after CHOP chemotherapy on day 4.

Twenty patients received rituximab ( $375 \text{ mg/m}^2$ ) in addition to CHOP (1). Rituximab was administered 1 day (group 1) or 2 days (group 2) before CHOP.

A baseline FLT-PET examination was done within 1 week before therapy, together with other staging modalities (clinical examination, CT) and FDG-PET. In group 1 ( $n = 6$ ), FLT-PET imaging was repeated at day 7 (range, day 6 to day 7; mean, 6.3) after the first course of R-CHOP (four patients) or CHOP (two patients). A third PET study ( $n = 4$ ) was done after completion of the second cycle of R-CHOP/CHOP at day 40 (range, day 38 to day 41; mean, 39.3). In group 2, all 16 patients received R-CHOP and underwent a second FLT-PET scan at day 2 (range, day 2 to day 3; mean, 2.3) after rituximab administration (day 0). Rituximab was administered without prior dexamethasone medication in 13 patients. In three patients, dexamethasone had to be given for medical reasons. In group 2, CHOP was given after the second FLT-PET (day 2). In this group, a third PET study was done 2 days after the first course of CHOP at day 4 (range, day 4 to day 6; mean, 4.4) in nine patients. After completion of three and six courses of R-CHOP, standard restaging procedures including morphologic imaging (CT or magnetic resonance imaging) were scheduled (see Fig. 1 for treatment schedule).

**PET imaging.** FLT was synthesized as previously described (37). Imaging was done on a whole-body high-resolution PET scanner (ECAT HR+, Siemens/CTI, Inc.). This device simultaneously acquires 47 contiguous slices with a slice thickness of 3.4 mm. The in-plane image resolution of transaxial images was  $\sim 8\text{-mm}$  full width at half maximum, with an axial resolution of  $\sim 5\text{-mm}$  full width at half maximum.

Static emission images were acquired 45 min after injection of  $\sim 300\text{-MBq}$  FLT (range, 270-340 MBq). Emission data were corrected for random coincidences, dead time, and attenuation, and reconstructed by filtered backprojection (Hanning filter with cutoff frequency of 0.4 cycle per bin). The matrix size was  $128 \times 128$  pixels with a pixel size of  $4.0 \times 4.0$  mm. The image pixel counts were calibrated to activity concentrations (Becquerel per milliliter) and decay corrected using the time of tracer injection as reference.

**PET data analysis.** All PET scans were evaluated by two observers blinded to the clinical data and the results of other imaging studies. Circular regions of interest with a diameter of 1.5 cm were placed in the area with the highest tumor activity, as previously published by Weber et al. (38). Mean lesion diameter and range of initial tumor size were 4.6 cm (median, 4.0; range, 2.0-17.5). Mean SUVs were calculated from each region of interest using the following formula:  $\text{SUV} = \text{measured activity concentration (Bq/g)} \times \text{body weight (g)} / \text{injected activity (Bq)}$ .

For further analyses, mean values from both observers were used. Regions of interest were also placed in following tissues: liver (right liver lobe, excluding the central part and the liver margins), bone marrow (lumbar vertebra four), and gluteal muscle. Side-by-side analysis has been done to ensure SUV calculation in identical regions of interest at various time points. This algorithm has been demonstrated to be a valuable tool for assessment of therapy response (38, 39).

For definition of regions of interest and data analysis, computer programs were developed in the Interactive Data Language (IDL; Research Systems, Inc.) using the Clinical Application Programming Package (CAPP; Siemens/CTI; ref. 40).

**Clinical evaluation and follow-up.** CT was done as part of the routine clinical management in all patients. Baseline CTs of head and neck, thorax, abdomen, and pelvis were done in all patients before chemotherapy. Patients were reevaluated by means of CT after three and six courses of chemotherapy. The treatment response was classified after completion of six cycles of R-CHOP/CHOP as complete response (CR), partial response (PR), no change, or progressive disease according to the Response Evaluation Criteria in Solid Tumors criteria published by Therasse et al. (41) based on the bidimensional diameters of corresponding tumor lesions measured by ruler or caliper. Further evaluations of treatment response were carried out according to standard protocols every 3 months. The patient management was not influenced by the results of FLT-PET studies.

**Statistical analysis.** Statistical analyses were done using SPSS software (version 14.0; SPSS, Inc.). Quantitative values were expressed as mean  $\pm 1$  SD. All tests ( $t$  test for related and independent samples and Mann-Whitney  $U$  test) were two sided and were done at the 5% level of statistical significance.

## Results

**Patients.** Eighteen patients had diffuse large B-cell non-Hodgkin's lymphoma (clinical stage IA-IVA; Table 1), two patients had grade 3 follicular lymphoma (both clinical stage IVA), and two patients had nodal anaplastic large T-cell non-Hodgkin's lymphoma (both clinical stage IIIA).

**Initial biodistribution of FLT.** FLT-PET produced images of high contrast of both lymphoma and proliferating bone marrow. In all patients, focal FLT uptake could be detected in lymphoma manifestation sites described by routine staging procedures (sensitivity of FLT-PET, 100%). Mean uptake of FLT

in lymphoma manifestations (mean FLT SUV) was 8.1 (median, 7.4; SD, 3.9; range, 2.6-19.4). Mean initial FLT uptake in lymphoma did not significantly vary between the two different groups (mean SUV value: group 1, 6.0; group 2, 9.0;  $P = 0.06$ ). Besides tracer accumulation in malignant lymphoma, high FLT uptake in bone marrow was observed (mean SUV value, 7.0; median, 6.8; range, 4.2-9.0). The mean FLT SUV in a reference segment of the liver was 4.7 (median, 4.4; range, 2.9-7.9); spleen, 2.2 (median, 2.1; range, 1.3-3.8); and muscle, 0.8 (median, 0.8; range, 0.5-1.1). Figures 2 and 3 illustrate the biodistribution of FLT.

**PET response assessment 7 and 40 days after R-CHOP/CHOP (group 1).** In group 1, mean uptake of FLT in lymphoma manifestations before therapy was 6.0 ( $n = 6$ ; median, 5.7; SD, 1.4; range, 4.6-8.2). Seven days after initiation of chemotherapy, FLT uptake in lymphoma was significantly reduced by 77% ( $n = 6$ ; mean SUV value, 1.4; median, 1.4; SD, 0.5; range, 0.7-2.0;  $P < 0.001$ ) and after 40 days by 85% ( $n = 4$ ; mean SUV value, 1.0; median, 0.9; SD, 0.3; range, 0.7-1.4) versus initial uptake (mean SUV value, 6.5; median, 6.6; SD, 1.5; range, 4.7-8.2;  $P = 0.003$ ). In contrast, FLT uptake in the liver remained stable over the time course and showed no significant alterations (mean SUV value, 4.2, 4.0, and 4.4, respectively). Seven days after initiation of chemotherapy, FLT uptake in the bone marrow showed a mild decrease (mean SUV value, 6.2 and 5.1;  $P = 0.42$ ) and returned to initial values at the later time point (mean SUV value, 6.8;  $P = 0.76$ ; Fig. 2).

**PET response assessment 2 days after rituximab and 2 days after CHOP (group 2).** Thirteen patients were evaluated according to the protocol of group 2; three patients received dexamethasone before rituximab and were therefore analyzed separately. Initial lymphoma FLT uptake in the patients without dexamethasone was 9.4 ( $n = 13$ ; median, 8.3; SD, 4.6; range, 2.6-19.4). All 13 patients underwent FLT-PET early after

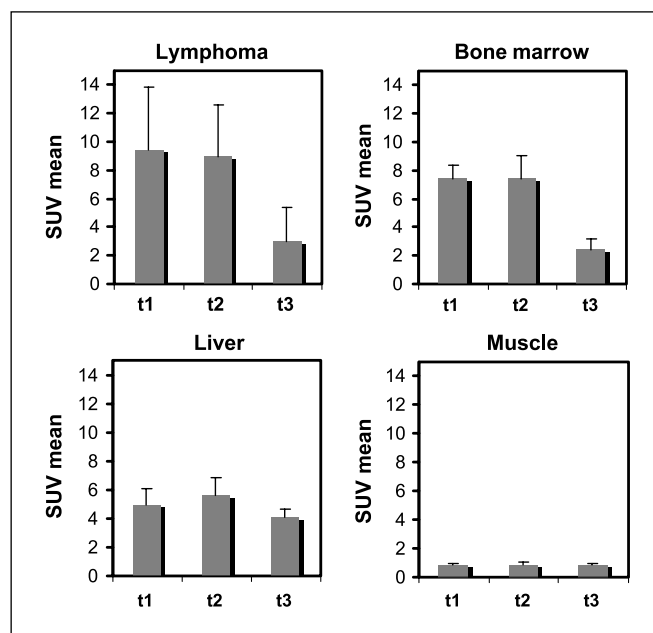


Fig. 3. Absolute mean SUVs of the indicated tissues during the treatment course of group 2 ( $n = 13$ ) without dexamethasone pretreatment before rituximab at baseline (t1), on day 2 (t2), and on day 4 (t3).

rituximab administration and revealed no significant change in lymphoma FLT uptake ( $n = 13$ ; mean SUV value, 8.9; median, 8.2; SD, 3.8; range, 2.5-16.3;  $P = 0.3$ ). In contrast, mean FLT uptake was significantly decreased 2 days after CHOP ( $n = 8$ ; mean SUV value, 3.0; median, 2.3; SD, 2.6; range, 1.0-9.0) versus initial uptake (mean SUV value, 9.4; median, 8.2; SD, 5.3; range, 2.6-19.4;  $P = 0.004$ ; Figs. 3 and 4). In the second PET, bone marrow uptake of FLT uptake was comparable to the initial uptake (mean SUV value, 7.4; day 2, 7.4;  $P = 0.93$ ), whereas it significantly decreased at time point 3 (2.4;  $P < 0.001$ ). FLT uptake in the liver remained stable over the different time points as described for group 1 (mean SUV value, 5.0, 5.6, and 4.1, respectively; Figs. 3 and 4).

In the three patients treated with dexamethasone before rituximab administration (patient nos. 12, 13, and 20), mean initial FLT uptake at lymphoma sites was 6.9 ( $n = 3$ ; median, 7.2; SD, 0.9; range, 5.8-7.6). Two days after administration of rituximab and dexamethasone, FLT uptake was significantly lower ( $n = 3$ ; mean SUV value, 2.4; median, 2.4; SD, 0.3; range, 2.1-2.7;  $P = 0.018$ ) compared with the initial FLT uptake. Bone marrow showed also a significant decrease between the two measurements (initial mean SUV value, 7.1; day 2, 2.2;  $P = 0.024$ ), whereas the values in the liver remained stable (initially 4.7; day 2, 4.2;  $P = 0.24$ ).

**Assessment of clinical response and follow-up.** Clinical response and follow-up were available in 21 of 22 patients; there was one non-lymphoma-related death (patient no. 11) during the first cycle of therapy (Table 1). After six cycles of R-CHOP/CHOP, clinical response was assessed by conventional imaging. During the first two cycles, one patient showed progressive disease (patient no. 10) and was switched to a salvage chemotherapy regimen. The remaining 20 patients responded to therapy and were rated as CR (14) or PR (6).

To date, median follow-up is 12.6 months in 20 patients (range, 3.3-24.2 months). Of 20 patients initially responding to

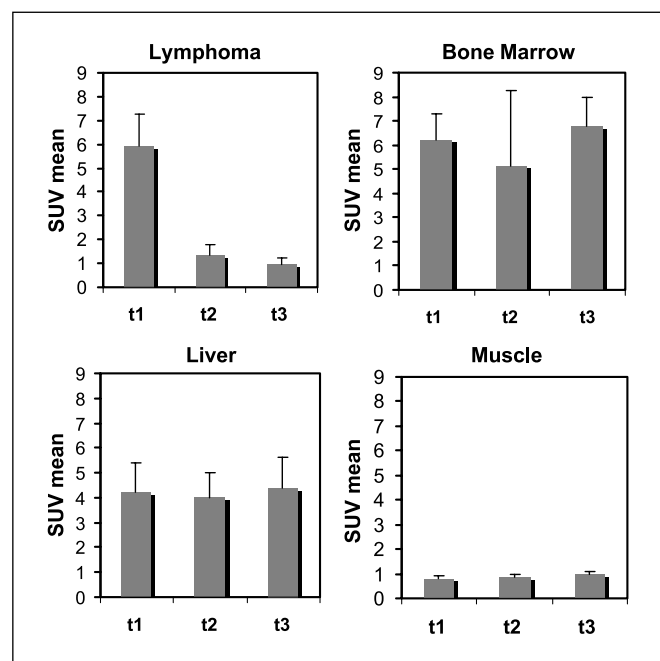


Fig. 2. Absolute mean SUVs of the indicated tissues during the treatment course of group 1 ( $n = 6$ ) at baseline (t1), on day 7 (t2), and on day 40 (t3).

therapy, 15 patients were rated as CR, 3 patients as PR, and 2 patients as relapse. One of the two patients with disease recurrence was initially in CR (patient no. 12) and the other one in PR (patient no. 2).

**Correlation of repetitive FLT-PET scans to clinical response and follow-up.** All patients responding to chemotherapy showed significant reduction of FLT uptake in lymphoma after administration of R-CHOP and the remaining FLT uptake was lower than liver uptake in all patients. In contrast, the patient with refractory disease revealed a high persisting FLT uptake at the lymphoma manifestation site with a modest decline of 39%, compared with the initial uptake (initial SUV value, 14.8; after R-CHOP, 9.0).

There was no statistically significant difference between initial FLT uptake in patients with PR or CR, as indicated by the CT scan ( $P = 0.09$ ). Interestingly, in the 14 patients receiving PET early after completion of the first cycle of chemotherapy ( $n = 8$ , 2 days after completion of R-CHOP;

$n = 6$ , 7 days after completion of R-CHOP/CHOP; patient no. 10 was excluded for progression), we were able to detect a marked difference in tumoral FLT retention between patients reaching PR versus CR (mean SUV value, 2.6 versus 1.5;  $P = 0.009$ ) at the end of therapy.

After a median follow-up of 12.6 months, the majority of patients were still in complete or partial remission ( $n = 18$ ). Only two patients developed relapse after initial response (patient no. 2, 67% decrease of initial FLT-uptake; patient no. 12, no FLT PET after completion of first cycle R-CHOP). Due to the low number of relapsed patients, correlation of FLT-PET scans to long-term outcome has not been done.

### Discussion

This is one of the first clinical studies indicating that early response assessment to chemotherapy with a molecular probe specifically addressing tumor proliferation is feasible.

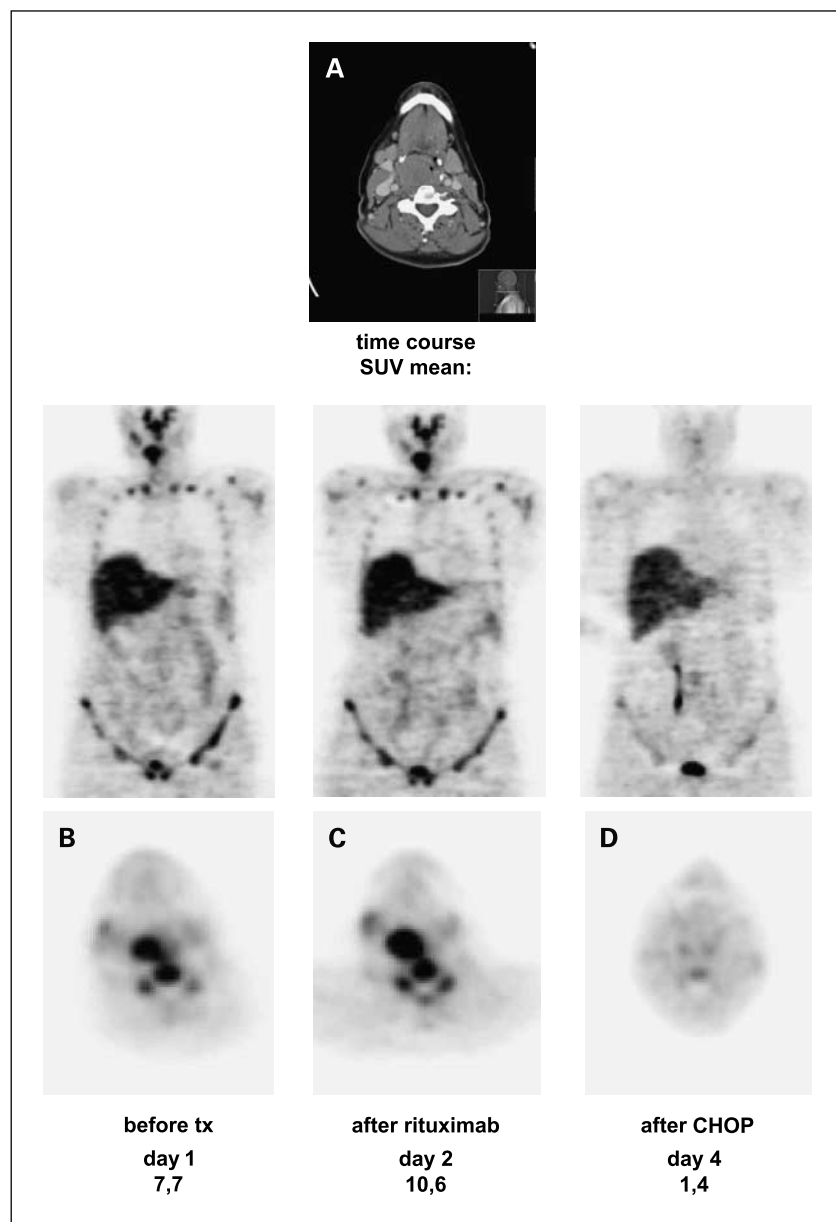


**Fig. 4.** Conventional CT (A) and FLT-PET scan at baseline (B) of the lymphoma region and coronal whole body image of patient no. 15 (group 2). C and D, corresponding FLT-PET images of the lymphoma region and the coronal whole body image during R-CHOP 2 d after rituximab (C) and 2 d after CHOP (D).



Recently, *in vitro* and animal studies already suggested the use of FLT for therapeutic monitoring (34). In an animal model of fibrosarcoma, it was reported that FLT uptake decreased early after antiproliferative treatment with 5-fluorouracil or cisplatin (42, 43). In a mouse lymphoma xenotransplant model, significant decrease of FLT uptake was observed already 48 h after chemotherapy with cyclophosphamide (34). FLT-PET is therefore a promising tool for evaluation of therapy response. Already 2 days after administration of R-CHOP, FLT uptake at lymphoma manifestation sites was significantly decreased in all responding patients, with a tumor-to-liver ratio <1. In contrast, one nonresponding patient revealed a high residual FLT uptake resulting in a tumor-to-liver ratio of 2 (mean SUV decrease of 39%). The first relapsed patient was in partial remission after six cycles of R-CHOP, which was correctly indicated by a significant decrease in FLT uptake (reduction, 67%). The second patient with recurrent disease did not receive a PET scan after completion of chemotherapy. These data indicate that FLT uptake is a surrogate marker for response to immunochemotherapy.

Interestingly, a difference in tumoral FLT uptake between patients in PR and CR could be observed in the 14 patients receiving a PET scan early after completion of chemotherapy ( $P = 0.009$ ). During follow-up, we observed one non-lymphoma-related death, one patient with refractory disease, and two patients with progressive disease after PR and CR, resulting in an overall response rate of 82% (18 of 22). This high response rate is in accordance with earlier treatment studies evaluating R-CHOP versus CHOP in high-grade lymphomas (1). Due to the low number of relapsed or refractory patients, the predictive value of FLT-PET could not be finally determined. This has to be examined in a study including a higher number of patients.

Response assessment by cellular proliferation imaging was studied at first by Shields et al. (44) who evaluated the thymidine-based tracer [ $^{11}\text{C}$ ]thymidine in six patients with small-cell lung cancer and high-grade sarcoma before and 1 week after the start of chemotherapy. Patients responding to chemotherapy showed a decline for both thymidine and FDG uptake, whereas in nonresponders the thymidine uptake was unchanged. Response to therapy as measured by FLT-PET has also been shown in breast cancer. In a clinical study of 14 patients, Pio et al. (31) showed that mean change in FLT uptake in primary and metastatic tumors already after one course of chemotherapy is significantly correlated with late changes in tumor marker levels.

Interestingly, FLT-PET imaging 2 days after administration of rituximab revealed unchanged FLT uptake in lymphoma manifestation sites. We were able to discriminate the rituximab effect on *in vivo* proliferation from that of CHOP administra-

tion, which indicates that rituximab alone is not able to induce an immediate antiproliferative effect. These findings are consistent with earlier studies which showed that rituximab as a single drug is not able to induce sufficient cytotoxicity in diffuse large B-cell lymphoma (3). The mechanism of action of rituximab is not completely understood. Thus far, three possible mechanisms of action have been discussed, all studied in isolated cells and cell lines: (a) direct induction of apoptosis by inhibition of major survival pathways, such as nuclear factor  $\kappa\text{B}$  and mitogen-activated protein kinases, and the induction of antiapoptotic proteins (i.e., bcl-2), and thus working synergistically with cytotoxic drugs; (b) antibody-dependent cellular cytotoxicity, mediated by Fc $\gamma$  receptor-expressing cells (monocytes, granulocytes, and natural killer cells), which in turn can recruit and activate T cells; and (c) induction of the complement cascade, which results in activation membrane attacking complex, leading to destruction of cell membranes (45).

As previously shown by other studies, FLT-PET has a high sensitivity in detecting lymphoma (32). In our study, lymphoma manifestation sites were detected with FLT-PET in all patients. However, several limitations have to be taken into account when transferring our results to the clinic. First, different types of therapy may cause alterations in the metabolism of FLT by increasing cellular efflux of FLT, altering activity of thymidine kinase 1 or increasing/decreasing cellular content of the cofactor ATP. Second, due to the limited number of patients included in this pilot study and the high response rates of these high-grade tumor entities, we were not able to draw final conclusions about the predictive value of changes in FLT uptake and long-term clinical response. Third, given the fact that FDG-PET has been introduced into standard imaging evaluations for monitoring malignant lymphoma, a significant benefit of FLT-PET imaging has to be shown in future studies. Fourth, whereas FLT seems to be more specific compared with FDG, unspecific tracer uptake in benign lesions with a high proliferation rate (e. g. sarcoidosis) cannot be excluded.

In conclusion, R-CHOP/CHOP leads to a rapid decrease of FLT uptake early in the course of therapy presumably due to a reduction of tumor cell proliferation. In contrast, rituximab administration alone leads to no significant change of FLT uptake, indicating no association with early antiproliferative effects. FLT-PET seems to be a promising, sensitive tool for quantitative assessment of various drug effects on tumor cell proliferation.

## Acknowledgments

We thank our colleagues Michael Fromm, M.D., and Burkhard Schmidt, M.D., for their excellent contributions and our technical staff members Brigitte Dzewas and Coletta Kruschke for their great support.

## References

1. Coiffier B, Lepage E, Briere J, et al. CHOP chemotherapy plus rituximab compared with CHOP alone in elderly patients with diffuse large-B-cell lymphoma. *N Engl J Med* 2002;346:235–42.
2. Pfreundschuh M, Trumper L, Osterborg A, et al. CHOP-like chemotherapy plus rituximab versus CHOP-like chemotherapy alone in young patients with good-prognosis diffuse large-B-cell lymphoma: a randomised controlled trial by the MabThera International Trial (MInT) Group. *Lancet Oncol* 2006;7:379–91.
3. Maloney DG, Grillo-Lopez AJ, Bodkin DJ, et al. IDEC-C2B8: results of a phase I multiple-dose trial in patients with relapsed non-Hodgkin's lymphoma. *J Clin Oncol* 1997;15:3266–74.
4. Bangert M, Moog F, Buchmann I, et al. Whole-body 2-[ $^{18}\text{F}$ ]-fluoro-2-deoxy-D-glucose positron emission tomography (FDG-PET) for accurate staging of Hodgkin's disease. *Ann Oncol* 1998;9:1117–22.
5. Jerusalem G, Beguin Y, Fassotte MF, et al. Whole-body positron emission tomography using  $^{18}\text{F}$ -fluoro-deoxyglucose compared to standard procedures for staging patients with Hodgkin's disease. *Haematologica* 2001;86:266–73.
6. Menzel C, Dobernt N, Mitrou P, et al. Positron emission tomography for the staging of Hodgkin's lymphoma-increasing the body of evidence in favor of the method. *Acta Oncol* 2002;41:430–6.
7. Mikhaeel NG, Timothy AR, O'Doherty MJ, Hain S, Maisey MN. 18-FDG-PET as a prognostic indicator in the treatment of aggressive Non-Hodgkin's Lymphoma-comparison with CT. *Leuk Lymphoma* 2000;39:543–53.

8. Naumann R, Beuthien-Baumann B, Reiss A, et al. Substantial impact of FDG PET imaging on the therapy decision in patients with early-stage Hodgkin's lymphoma. *Br J Cancer* 2004;90:620–5.
9. Partridge S, Timothy A, O'Doherty MJ, Hain SF, Rankin S, Mikhaeel G. 2-Fluorine-18-fluoro-2-deoxy-D-glucose positron emission tomography in the pretreatment staging of Hodgkin's disease: influence on patient management in a single institution. *Ann Oncol* 2000;11:1273–9.
10. Wehrauch MR, Re D, Bischoff S, et al. Whole-body positron emission tomography using  $^{18}\text{F}$ -fluorodeoxyglucose for initial staging of patients with Hodgkin's disease. *Ann Hematol* 2002;81:20–5.
11. Jerusalem G, Beguin Y, Fassotte MF, et al. Whole-body positron emission tomography using  $^{18}\text{F}$ -fluorodeoxyglucose for posttreatment evaluation in Hodgkin's disease and non-Hodgkin's lymphoma has higher diagnostic and prognostic value than classical computed tomography scan imaging. *Blood* 1999;94:429–33.
12. Moog F, Bangertner M, Diederichs CG, et al. Lymphoma: role of whole-body 2-deoxy-2-[ $^{18}\text{F}$ ]fluoro-D-glucose (FDG) PET in nodal staging. *Radiology* 1997;203:795–800.
13. Moog F, Bangertner M, Diederichs CG, et al. Extrnodal malignant lymphoma: detection with FDG PET versus CT. *Radiology* 1998;206:475–81.
14. Mikhaeel NG, Hutchings M, Fields PA, O'Doherty MJ, Timothy AR. FDG-PET after two to three cycles of chemotherapy predicts progression-free and overall survival in high-grade non-Hodgkin lymphoma. *Ann Oncol* 2005;16:1514–23.
15. Jerusalem G, Beguin Y, Fassotte MF, et al. Early detection of relapse by whole-body positron emission tomography in the follow-up of patients with Hodgkin's disease. *Ann Oncol* 2003;14:123–30.
16. Romer W, Hanauske AR, Ziegler S, et al. Positron emission tomography in non-Hodgkin's lymphoma: assessment of chemotherapy with fluorodeoxyglucose. *Blood* 1998;91:4464–71.
17. Spaepen K, Stroobants S, Dupont P, et al. Early restaging positron emission tomography with ( $^{18}\text{F}$ )F-fluorodeoxyglucose predicts outcome in patients with aggressive non-Hodgkin's lymphoma. *Ann Oncol* 2002;13:1356–63.
18. Juweid ME, Cheson BD. Positron-emission tomography and assessment of cancer therapy. *N Engl J Med* 2006;354:496–507.
19. Juweid ME, Stroobants S, Hoekstra OS, et al. Use of positron emission tomography for response assessment of lymphoma: consensus of the Imaging Subcommittee of International Harmonization Project in Lymphoma. *J Clin Oncol* 2007;25:571–8.
20. Juweid ME, Wiseman GA, Vose JM, et al. Response assessment of aggressive non-Hodgkin's lymphoma by integrated International Workshop Criteria and fluorine-18-fluorodeoxyglucose positron emission tomography. *J Clin Oncol* 2005;23:4652–61.
21. Kubota R, Kubota K, Yamada S, Tada M, Ido T, Tamahashi N. Microautoradiographic study for the differentiation of intratumoral macrophages, granulation tissues and cancer cells by the dynamics of fluorine-18-fluorodeoxyglucose uptake. *J Nucl Med* 1994;35:104–12.
22. Shreve PD, Anzai Y, Wahl RL. Pitfalls in oncologic diagnosis with FDG PET imaging: physiologic and benign variants. *Radiographics* 1999;19:61–77; quiz 150–1.
23. Buck AC, Schirrmeyer HH, Guhlmann CA, et al. Ki-67 immunostaining in pancreatic cancer and chronic active pancreatitis: does *in vivo* FDG uptake correlate with proliferative activity? *J Nucl Med* 2001;42:721–5.
24. Shields AF, Grierson JR, Dohmen BM, et al. Imaging proliferation *in vivo* with [ $^{18}\text{F}$ ]FLT and positron emission tomography. *Nat Med* 1998;4:1334–6.
25. Barthel H, Perumal M, Latigo J, et al. The uptake of 3'-deoxy-3'-[ $^{18}\text{F}$ ]fluorothymidine into L5178Y tumours *in vivo* is dependent on thymidine kinase 1 protein levels. *Eur J Nucl Med Mol Imaging* 2005;32:257–63.
26. Rasey JS, Grierson JR, Wiens LW, Kolb PD, Schwartz JL. Validation of FLT uptake as a measure of thymidine kinase-1 activity in A549 carcinoma cells. *J Nucl Med* 2002;43:1210–7.
27. Buck AK, Bommer M, Stilgenbauer S, et al. Molecular imaging of proliferation in malignant lymphoma. *Cancer Res* 2006;66:11055–61.
28. Buck AK, Halter G, Schirrmeyer H, et al. Imaging proliferation in lung tumors with PET:  $^{18}\text{F}$ -FLT versus  $^{18}\text{F}$ -FDG. *J Nucl Med* 2003;44:1426–31.
29. Cobben DC, Elsinga PH, Suurmeijer AJ, et al. Detection and grading of soft tissue sarcomas of the extremities with ( $^{18}\text{F}$ )F-3'-fluoro-3'-deoxy-L-thymidine. *Clin Cancer Res* 2004;10:1685–90.
30. Kenny LM, Vigushin DM, Al-Nahhas A, et al. Quantification of cellular proliferation in tumor and normal tissues of patients with breast cancer by [ $^{18}\text{F}$ ]fluorothymidine-positron emission tomography imaging: evaluation of analytical methods. *Cancer Res* 2005;65:10104–12.
31. Pio BS, Park CK, Pietras R, et al. Usefulness of 3'-[ $^{18}\text{F}$ ]fluoro-3'-deoxythymidine with positron emission tomography in predicting breast cancer response to therapy. *Mol Imaging Biol* 2006;8:36–42.
32. Wagner M, Seitz U, Buck A, et al. 3'-[ $^{18}\text{F}$ ]fluoro-3'-deoxythymidine ([ $^{18}\text{F}$ ]-FLT) as positron emission tomography tracer for imaging proliferation in a murine B-Cell lymphoma model and in the human disease. *Cancer Res* 2003;63:2681–7.
33. Choi SJ, Kim JS, Kim JH, et al. [ $^{18}\text{F}$ ]3'-deoxy-3'-Fluorothymidine PET for the diagnosis and grading of brain tumors. *Eur J Nucl Med Mol Imaging* 2005;32:653–9.
34. Buck AK, Vogg ATJ, Glatting G, Reske SN.  $^{18}\text{F}$ -FLT for monitoring response to antiproliferative therapy in a mouse lymphoma xenotransplant model. *J Nucl Med* 2004;45(suppl):154.
35. Dittmann H, Dohmen BM, Kehlbach R, et al. Early changes in [ $^{18}\text{F}$ ]FLT uptake after chemotherapy: an experimental study. *Eur J Nucl Med Mol Imaging* 2002;29:1462–9.
36. Jaffe ES, Harris NL, Stein H, Vardiman JH. World Health Organization classification of tumors. Pathology and genetics. Tumors of haematopoietic and lymphoid tissues. 2001.
37. Machulla HJ, Blocher A, Kuntzsch M, Piert M, Wei R, Grierson J. Simplified labeling approach for synthesizing 3'-deoxy-3'-[ $^{18}\text{F}$ ]fluorothymidine ([ $^{18}\text{F}$ ]FLT). *J Radioanal Nucl Chem* 2000;243:4.
38. Weber WA, Ott K, Becker K, et al. Prediction of response to preoperative chemotherapy in adenocarcinomas of the esophagogastric junction by metabolic imaging. *J Clin Oncol* 2001;19:3058–65.
39. Wieder HA, Brucher BL, Zimmermann F, et al. Time course of tumor metabolic activity during chemoradiotherapy of esophageal squamous cell carcinoma and response to treatment. *J Clin Oncol* 2004;22:900–8.
40. Weber WA, Ziegler SI, Thodtmann R, Hanauske AR, Schwaiger M. Reproducibility of metabolic measurements in malignant tumors using FDG PET. *J Nucl Med* 1999;40:1771–7.
41. Therasse P, Arbutnot SG, Eisenhauer EA, et al. New guidelines to evaluate the response to treatment in solid tumors. European Organization for Research and Treatment of Cancer, National Cancer Institute of the United States, National Cancer Institute of Canada. *J Natl Cancer Inst* 2000;92:205–16.
42. Barthel H, Cleij MC, Collingridge DR, et al. 3'-deoxy-3'-[ $^{18}\text{F}$ ]Fluorothymidine as a new marker for monitoring tumor response to antiproliferative therapy *in vivo* with positron emission tomography. *Cancer Res* 2003;63:3791–8.
43. Leyton J, Latigo JR, Perumal M, Dhaliwal H, He Q, Aboagye EO. Early detection of tumor response to chemotherapy by 3'-deoxy-3'-[ $^{18}\text{F}$ ]fluorothymidine positron emission tomography: the effect of cisplatin on a fibrosarcoma tumor model *in vivo*. *Cancer Res* 2005;65:4202–10.
44. Shields AF, Mankoff DA, Link JM, et al. Carbon-11-thymidine and FDG to measure therapy response. *J Nucl Med* 1998;39:1757–62.
45. Jazirehi AR, Bonavida B. Cellular and molecular signal transduction pathways modulated by rituximab (rituxan, anti-CD20 mAb) in non-Hodgkin's lymphoma: implications in chemosensitization and therapeutic intervention. *Oncogene* 2005;24:2121–43.